Carbon Nanotube Growth on a Swellable Clay Matrix

A. Bakandritsos, A. Simopoulos, and D. Petridis*

Institute of Materials Science, National Center for Scientific Research (NCSR) "Demokritos", Agia Paraskevi, 15310, Athens, Greece

Received October 12, 2004. Revised Manuscript Received April 4, 2005

The successful growth of multiwalled carbon nanotubes on montmorillonite surfaces has been attained via chemical vapor deposition of acetylene and studied by means of electron microscopy, XRD, Mössbauer spectroscopy, and thermal analysis measurements. Clay surfaces loaded with different amounts and types of metal salt catalyst precursors, namely $FeCl_3 \cdot 6H_2O$, $Fe(NO_3)_3 \cdot 9H_2O$, $Ni(NO_3)_2 \cdot 6H_2O$, and $Co(NO_3)_2 \cdot 6H_2O$, afforded clay−carbon nanotube composite products with varying carbon nanotube content and quality. The anion of the metal salt controls the hydrolysis during metal deposition on the clay surfaces and affects the transition to metal carbides at the final step of carbon deposition. Replacement of iron chloride by iron nitrate induced a minimum content of carbide impurities in the final product; nickel nitrate proved to be the best catalyst for nanotube growth, greatly improving their quality. Finally, the optimum time for carbon deposition at 700 °C and catalyst loading were elaborated in order to receive clay−carbon nanotube composites combining a high quality and appropriate content of carbon nanotube with the swelling, intercalation, and ion exchange properties of the parent mineral.

Introduction

The outstanding mechanical, electrical, and chemical properties of carbon nanotubes (CNs) have motivated extensive research for their synthesis, functionalization, and potential applications.[1] Particularly, in the field of synthesis, studies are focused on three main approaches: laser ablation,[2] carbon arc discharge,[3,4] and catalytic chemical vapor deposition (CVD).[5,6] Despite the fact that the two first methods produce CNs in high yield, especially single-walled CNs with a narrow diameter distribution, CVD has steadily gained ground because it is very simple and cost-effective. Moreover, the utilization of CVD in conjunction with patterned catalyst arrays affords mainly unbundled CNs, because of their growth from specific surface sites[5,7−9] unlike the other techniques.

The quality, yield, and nature of CNs produced by the CVD approach are influenced by many parameters including the carbon feeding gas, temperature of carbon deposition, nature of the catalyst, and the catalyst support. CO,[10,11] CH_4,[12−14] and C_2H_2[15] are the most common carbon sources, among others less widespread such as ethylene[11] and propylene.[15] Carbon monoxide and methane are believed to favor the formation of SWCNTs,[11,13,14] while C_2H_2 affords mainly multiwalled CNs[15] (MWCNs). Numerous metallic catalysts derived from reduction of transition state metal salts, such as $FeCl_3$,[5] $Fe(NO_3)_3$ and $FeSO_4$,[13] $Ni(NO_3)_2$,[16] and $Ni(HCOO)_2$,[17] have been employed, as well as Fe or Co/MgO mixed oxide powders.[6] Doping of catalysts with other metals, such as Mo or Ru, has also been reported as promoting the quality of the products.[18,19] The catalysts are supported on high-surface-area solids, such as alumina,[11] silica,[19,20] mesoporous silica,[21] and zeolites.[22]

* To whom all correspondence should be addressed. E-mail: dpetrid@ims.demokritos.gr. Tel: 003 21065003343. Fax: 0032106519430.

(1) Dresselhaus, M. S.; Dresselhaus, G.; Avouris, Ph. *Carbon Nanotubes Synthesis, Structures, and Applications*; Springer: Berlin, New York, 2001.
(2) Rinzler, A. G.; Liu, J.; Dai, H.; Nikolaev, P.; Huffman, C. B.; Rodriguez-Macias, F. J.; Boul, P. J.; Lu, A. H.; Heyman, D.; Colbert, D. T.; Lee, R. S.; Fischer, J. E.; Rao, A. M.; Eklund, P. C.; Smalley, R. E. *Appl. Phys. A* **1998**, *67*, 29.
(3) Iijima, S. *Nature* **1991**, *354*, 56.
(4) Journet, C.; Maser, W. K.; Bernier, P.; Loiseau, A.; de la Chapelle, M. L.; Lefrant, S.; Lee, R.; Fischer, J. E. *Nature* **1997**, *388*, 756.
(5) Hou, H.; Schaper, A. K.; Jun, Z.; Weller, F.; Greiner, A. *Chem. Mater.* **2003**, *15*, 580−585.
(6) Coquay, P.; Peigney, A.; De Grave, E.; Vandenberghe, R. E.; Laurent, C. *J. Phys. Chem. B* **2002**, *106*, 13199.
(7) Hongjie, D. *Acc. Chem. Res.* **2002**, *35*, 1035−1044.
(8) Flahaut, E.; Peigney, A.; Laurent, Ch.; Rousset, A. *J. Mater. Chem.* **2000**, *10*, 249.
(9) Bacsa, R. R.; Laurent, Ch.; Peigney, A.; Bacsa, W. S.; Vaugien, Th.; Rousset, A. *Chem. Phys. Lett.* **2000**, *323*, 566.
(10) Alvarez, W. E.; Pompeo, F.; Herrera, J. E.; Balzano, L.; Resasco, D. E. *Chem. Mater.* **2002**, *14*, 1853.
(11) Hafner, J. H.; Bronikowski, M. J.; Azamian, B. R.; Nikolaev, P.; Rinzler, A. G.; Colbert, D. T.; Smith, K. A.; Smalley, R. E. *Chem. Phys. Lett.* **1998**, *296*, 195.
(12) Harutyunyan, A. R.; Pradhan, B. K.; Kim, U. J.; Chen, G.; Eklund, P. C, *Nano Lett.* **2002**, *2* (5), 525.
(13) Cassell, A. M.; Raymakers, J. A.; Kong, J.; Dai, H. *J. Phys. Chem. B* **1999**, *103*, 6484.
(14) Zhang, Y.; Li, Y.; Kim, W.; Wang, D.; Dai, H. *Appl. Phys. A* **2002**, *74*, 325.
(15) Hernadi, K.; Fonseca, A.; Nagy, J. B.; Bernaerts, D.; Loukas, A. A *Carbon* **1996**, *34* (10), 1249.
(16) Park, C.; Keane, M. A. *J. Colloid Interface Sci.* **2002**, *250*, 37.
(17) Geng, J.; Singh, C.; Shephard, D. S.; Shaffer, M. S. P.; Johnson, B. F. G.; Windle, A. H. *Chem. Commun.* **2002**, 2666.
(18) Harutyunyan, A. R.; Pradhan, B. K.; Kim, U. J.; Chen, G.; Eklund, P. C. *Nano Lett.* **2002**, *2* (5), 525.
(19) Alvarez, W. E.; Pompeo, F.; Herrera, J. E.; Balzano, L.; Resasco, D. E. *Chem. Mater.* **2002**, *14*, 1853.
(20) Wei, B. Q.; Zhang, Z. J.; Ajayan, P. M.; Ramanath, G. *Carbon* **2002**, *40*, 47.
(21) Zheng, F.; Liang, L.; Gao, Y.; Sukamto, J. H.; Aardahl, C. L. *Nano Lett.* **2002**, *2* (7), 729.
(22) Zhang, A.; Li, C.; Bao, S.; Xu, Q. *Microporous Mesoporous Mater.* **1999**, *29*, 383.

10.1021/cm0482131 CCC: $30.25
Published on Web 05/20/2005

Recently, the growth of MWCNs by CVD of C_2H_2 on an Fe(III) exchanged montmorillonite substrate was reported.[23] Montmorillonite belongs to the family of naturally occurring 2:1 aluminosilicate smectite minerals with a single octahedral layer lying between two tetrahedral layers, altogether forming the clay platelet. Smectites have unique swelling, intercalation, and ion exchange properties that enable their restructuring into various valuable derivatives.[24] Growth of CNs on montmorillonite layers could provide another interesting class of materials for potential application in polymer reinforcement,[25] electrochemical energy production and storage,[26] and sensors.[27] It is now well established that small amounts (∼5%) of exfoliated montmorillonite in polymers enhances their mechanical, thermal, and other properties.[28] On the other side, CNs exhibit the highest Young's modulus and tensile strength among all materials.[29] Nevertheless, there are certain obstacles for the successful utilization of CNs in polymer reinforcing, emerging mostly from their self-assembly in bundles[30] and from poor grafting to the polymer chains. For these reasons, it is worth investigating if these drawbacks, causing inadequate dispersion in the polymer mass and poor load transfer across the CN-polymer interface, could be partially alleviated by exploiting the unique properties of clays in their respective composites. Specifically, exfoliated clay layers in a polymer could carry along their CN partners and, potentially, promote their adequate dispersion. As known, clay layers exfoliate spontaneously in hydrophilic polymers,[31] but for organophilic polymers organic modification of their surfaces is needed.[32] In the same sense analogous surface modification is needed for the successful exfoliation of the clay−CN hybrids in organophilic polymers.

Aiming at these potentialities, the present work seeks the optimum conditions for the synthesis of swellable clay−CN composites with an appropriate content and high quality of nanotubes, by studying certain parameters that affect deposition, quality, and yield of CNs. Simultaneously, preserving the mineral properties in the final composites is a crucial factor for their effective use in tri-phase polymeric composite materials and in other applications.

Experimental Section

Materials and Synthetic Procedure. The montmorillonite used in this study was from the island of Milos, Greece, with the code name Zenith-N. According to the supplier, Silver and Barytine Co., it contains 85% montmorillonite, 5% feldspars, 3% calcite, 2.5% quartz, 2% illite, and 2% cristobalite. The sample was fractionated to 2 μm by gravity sedimentation and purified by standard methods.[33] Most of the contaminants were removed during purification. The cation-exchange capacity of Na^+-montmorillonite is equal to 80 mequiv/100 g.

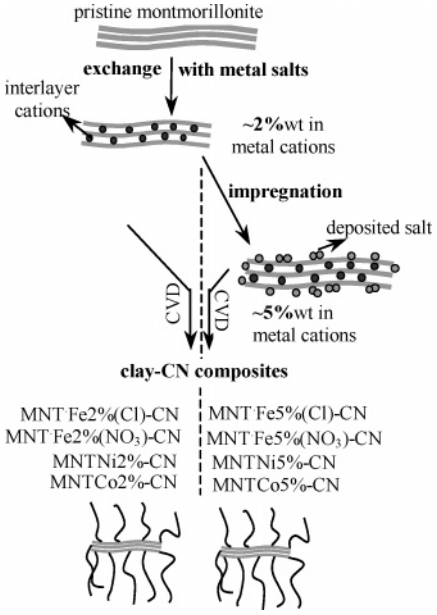

Figure 1. Schematic representation of the synthetic procedure leading to the final clay−carbon nanotube composites. Coding of products is also indicated.

The catalyst precursors were metal salts of $FeCl_3 \cdot 6H_2O$, $Fe(NO_3)_3 \cdot 9H_2O$, $Ni(NO_3)_2 \cdot 6H_2O$, and $Co(NO_3)_2 \cdot 6H_2O$. The catalyst precursors were deposited onto the clay substrate by two different procedures. The first includes an ion exchange reaction, in which the sodium cations of the parent clay were exchanged by the desired metal cations after mixing a clay suspension with an aqueous solution of the metal salt. The amount of the metal salt used in the exchange reactions was equivalent to three times the cation exchange capacity of montmorillonite. After 15 min of stirring, the mixture was centrifuged and washed with water. The procedure was repeated 3 times to secure complete exchange of the pristine sodium cations. The amount of metal cations deposited by the cation exchange technique is roughly 2 wt %.

To achieve higher metal loadings the already metal-exchanged montmorillonite was impregnated with aqueous solutions of metal salts in known concentrations. In this way, part of the metal ions occupied the exchange sites of the mineral and the rest deposited on the external surfaces as metal salts (Figure 1).

The metal ion exchanged or metal salt impregnated clay precursors were then inserted into a fixed bed flow reactor furnace and degassed at 80 °C with Ar for 20 min. The temperature was raised to 700 °C and then a mixture of Ar/C_2H_2 15% in C_2H_2 was introduced. A total flow rate of 45 mL/min was kept constant for various periods of time. The composite products after CVD treatment turned black due to the carbon deposition. Purification of the composites was attained by treatment in 2 M hot (70 °C) HNO_3 for 3 h to dispose of the metal catalyst particles. The pure CN component was obtained by treating the composite with a mixture of HF/HCL (approximately 8% w/w in each acid) which removes the clay framework. The clay precursors and the clay−

(23) Gournis, D.; Karakassides, M. A.; Bakas, T.; Boukos, N.; Petridis, D. *Carbon* **2002**, *40*, 2641.
(24) Nweman, A. C. D. *Chemistry of Clays and Clay Minerals;* Mineralogical Society Monograph No. 6; John Wiley & Sons: New York, 1987.
(25) Velasco-Santos, C.; Martýñez-Hernàndez, A. L.; Fisher, F. T.; Ruoff, R.; Castaño, V. M. *Chem. Mater.* **2003**, *15*, 4470.
(26) Che, G.; Lakshmi, B. B.; Fisher, E. R.; Martin, C. R. *Nature* **1998**, *393*, 346.
(27) Wong, S. S.; Jodelevich, E.; Woolley, A. T.; Cheung, C. L.; Lieber, C. M. *Nature* **1998**, *394*, 52.
(28) (a) Pinnavaia, T. J.; Beall, G. W., Eds. *Polymer-Clay Nanocomposites*; John Wiley & Sons Ltd.: New York, 2000. (b) Giannelis, E. P. *Adv. Mater.* **1996**, *8*, 29.
(29) (a) Ajayan, P. M.; Stephan, O.; Colliex, C.; Trauth, D. *Science* **1994**, *265*, 1212. (b) Ajayan, P. M.; Schadler, L. S.; Giannaris, C.; Rubio, A. *Adv. Mater.* **2000**, *12*, 750.
(30) Ajajan, P. M. *Chem. Rev.* **1999**, *99*, 9I, 1787.
(31) Vaia, R. A.; Vasudevan, S.; Krawiec W.; Scanlon L. G.; Giannelis, E. P. *Adv. Mater.* **1995**, *7* (2), 154.
(32) Alexandre, M.; Dubois, Ph. *Mater. Sci. Eng.* **2000**, *28*, 1.
(33) King, R. D.; Noceda, D. G.; Pinnavaia, T. J. *Electroanal. Chem.* **1987**, *236*, 43.

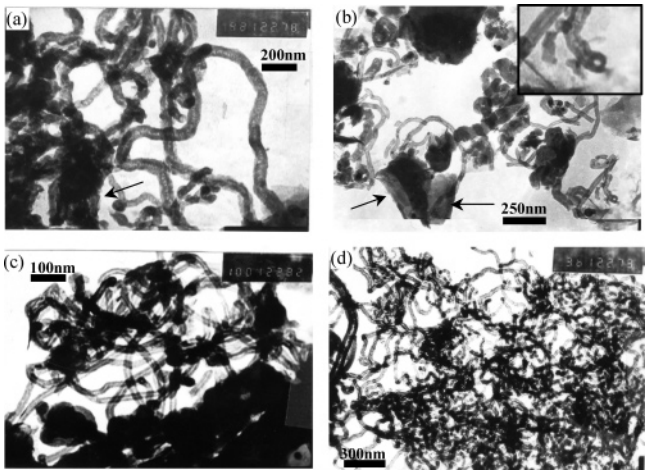

Figure 2. TEM images from clay−CN composites with (a) Fe as catalyst, (b) Co as catalyst, and (c) and (d) Ni as catalyst

CN composites are coded as MNT·M% in the former and as MNT·M%-CN in the latter case (MNT = montmorillonite, M = metal cation). When $FeCl_3 \cdot 6H_2O$ or $Fe(NO_3)_3 \cdot 9H_2O$ is used as precursor the anion is indicated in parentheses, e.g., MNT·Fe5%(NO_3)−CN.

The mineral properties in the final composites were tested by monitoring the increase in the basal spacing after subjecting them to treatment with vapors of ethylene glycol or diethylamine and with an aqueous solution of hexadecyl-trimethylammonium bromide. In the latter case, thorough washing after the exchange reaction ensures that the increase in the basal spacing arises solely from the electrostatically bound surfactant molecules.

Characterization. X-ray diffraction powder analysis was performed on a Siemens D-500 diffractometer with Cu Kα radiation. Transmission electron microscopy (TEM) was performed on a Philips CM20 electron microscope with applied acceleration voltage of 200 kV. Thermal analysis measurements were conducted under pure O_2 flow with a temperature ramp of 10 °C/min on a Perkin-Elmer thermogravimetric/differential analyzer. Mössbauer spectra were recorded by using a constant acceleration spectrometer with a 50 mCi ^{57}Co(Rh) source moving at room temperature, while the sample was placed in a variable-temperature cryostat. Isomer shift values are reported with respect to α-Fe.

Results and Discussion

Electron Microscopy. The growth of MWCNs by CVD of C_2H_2 upon Fe(III), Ni(II), and Co(II) loaded montmorillonite is clearly seen in the TEM micrographs in Figure 2. The hollow nature of the carbon tubes produced is evident in all systems. The mean diameter of the MWCNs was estimated at approximately 50−60 nm in the case of iron, ∼35 nm in the case of Co, and 20 nm in the case of Ni-grown nanotubes. The dark areas in the images correspond mainly to clay platelets. The arrows point to clay platelets where immobilized metal catalyst particles formulate the active centers for nanotube growth.

XRD Characterization. The XRD results from the derived composites provide a first evidence that the type of metal salt catalyst precursor affects the interaction between metal particles and carbon atoms at 700 °C. Specifically, in Figure 3a, the XRD pattern from the MNTFe5%(Cl)−CN composite contains reflections from the formation of the iron-carbide phase (Fe_3C), whereas these reflections are absent from the corresponding pattern of the MNTFe5%(NO_3)−

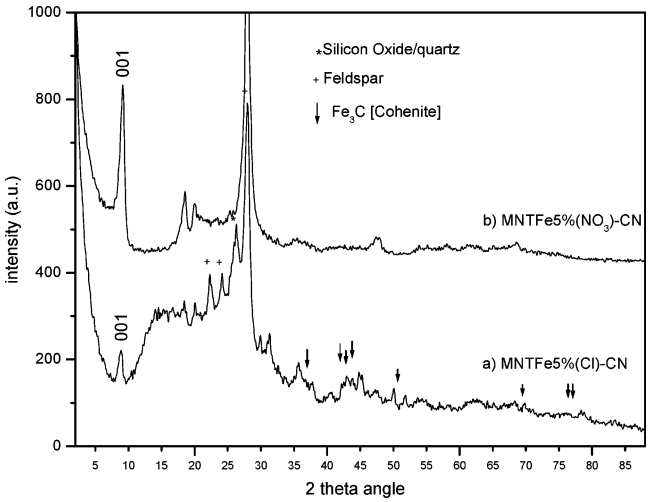

Figure 3. XRD patterns of the clay−CN composites: (a) MNTFe5%-(Cl)−CN and (b) MNTFe5%(NO_3)−CN.

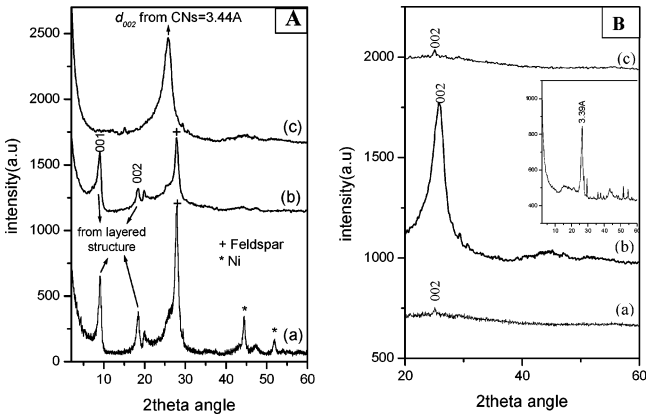

Figure 4. (A) XRD patterns from (a) MNTNi5%−CN composite, (b) the same composite after removal of catalyst impurities (Ni particles), and (c) the pure CN phase after dissolution of the clay. (B) XRD patterns of (a) Fe-, (b) Ni-, and (c) Co-grown multiwalled CNs after dissolution of the clay substrate. Inset: reflection at 3.39 Å from the multiwalled structure of commercial CNs, along with reflections from metal catalysts' presence.

CN composite. This is a notable result because metal carbides resist dissolution and therefore their removal from the clay−CN composites is a difficult operation. In addition, the X-ray diffractograms show that in both cases the 001 peak of the layered mineral is still present, even after 1 h treatment at 700 °C, reflecting the preservation of the lamellar aluminosilicate lattice.

The XRD patterns of the final clay−CN composites show the presence of the metal catalyst particles as, for instance Ni particles in the case of MNTNi5%−CN, in Figure 4A-(a). Such metal impurities in the composites can be removed after treatment with 2 M HNO_3 at 60 °C for 3 h as indicated in Figure 4A(b). A notable XRD result was obtained after dissolution of the mineral substrate. The XRD pattern of the remaining CNs, shown in Figure 4A(c), revealed the presence of a reflection at 3.44 Å. This peak, assigned to the d_{002} basal spacing of the concentric graphitic tubes in the MWCN framework, is an important marker for the formation of MWCNs. It is present in all MWCNs grown from the three different catalysts (Figure 4B), but only for the nickel-grown nanotubes is it intense and well-developed. It is scarcely distinguishable from the background noise for the Fe- and Co-grown MWCNs, although the same sample mass was

used in all measurements. In addition, it is noticed that the sharpness and intensity of the 002 reflection is accompanied by a lowering of the d_{002} basal spacing which approaches the value of 3.34 for ideal graphite. For instance, Ni-catalyzed CNs show a $d_{002} = 3.44$ Å, while CNs from Fe and Co give a $d_{002} = 3.51$ Å (Figure 4B(a and c)), and commercial MWCNTs give a $d_{002} = 3.39$ Å (inset Figure 4B).

The d_{002} basal spacing of the MWCN walls could provide a simple criterion for the CN quality because it can be correlated with the perturbation introduced by defects in the fine development of the concentric graphitic tubes, i.e., the fewer defects allow the d_{002} value to approach that of ideal graphite. This criterion is supported by the TG results as will be discussed below, because the number of defects is also correlated with the tube stability upon oxidation.[34]

Properties of Montmorillonite in the Clay−CN Composites. Seeking the optimum conditions for producing clay−CN composites, which retain to a great extent the exchange, swelling, and intercalation properties of the clay partner, attempts were made to prop the clay layers apart in the composites by intercalation of neutral molecules, such as ethylene glycol, ethylenediamine, or positively charged hexadecyltrimethylammonium bromide ($HTMA^+$). These attempts were not successful for composites obtained after 1 h CVD. However, when CVD was limited to 20 min, the obtained MNTFe5%(NO_3)−CN and MNTNi5%−CN composites were readily expanded, as seen by the increased d_{001} basal spacing of clay layers in Figure 5. These XRD results offer clear evidence for the insertion of these species into the lamellar space of montmorillonite. In particular, the insertion of $HTMA^+$ in the clay layers, even with washing after the exchange reaction, proves that the mineral keeps its cation exchange properties and its swelling ability. Here, we must also note that it appears that carbon formation over clay layers not only offers extra stability to its structure,[35] but also to the clay properties because when a metal-loaded clay sample was subjected to heat treatment at 700 °C without CVD, the swelling was very poor or not possible at all. Another important finding is the facile intercalation of the hydrophilic polyethylenoxide (PEO) into the clay−CN composite. In a relevant experiment, 2 mg of PEO was added to an aqueous suspension (15 mL, 0.2 wt %) of the MNTNi5%−CN composite and stirred for several hours. The observed basal spacing of 18 Å, Figure 5e, indicates the insertion of the polymer chains between the clay layers.[31] It is also noteworthy that composites with metal loadings higher than 5% and 20 min CVD did not expand the clay layers, probably because of the high CN content.

Thermogravimetric Measurements. TG/DTA measurements from the final clay−CN composites can survey the carbon content of the obtained composites and also the quality of the CNs produced, since their oxidation temperature is strongly influenced by the presence of wall defects.[34] Ideal graphite starts to oxidize above 600 °C[36] while CNs

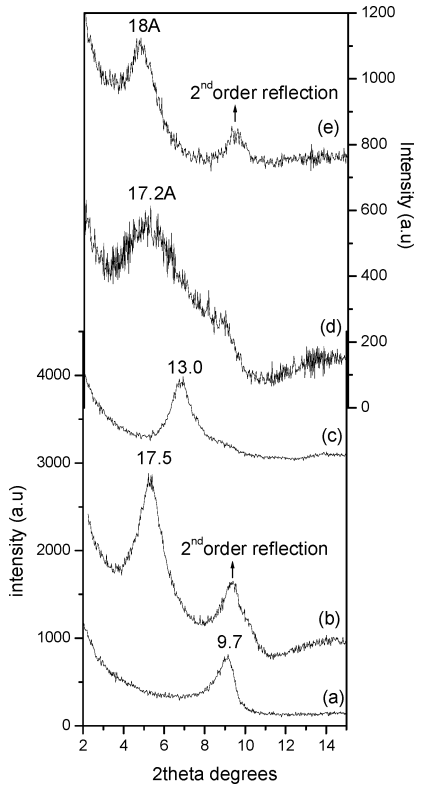

Figure 5. XRD patterns from the (a) as-prepared MNTNi5%−CN composite, (b) the latter after treatment with ethylene glycol vapors, (c) after treatment with ethylene-diamine vapors, (d) after treatment with aqueous solution of hexadecyl-trimethylammonium bromide and thorough washing, and (e) clay−CN composite after wet intercalation of polyethylenoxide (PEO).

are oxidized above 500 °C.[17] A first conclusion from thermogravimetric results is that increasing the catalyst loading from ∼2% to 5% affords composites with a CN content 2.5 times higher, as indicated by the thermograms in Figure 6b and c corresponding to 2% and 5% of Fe(III) loading. The choice of iron or nickel nitrate as metal salt precursors did not affect the CN yield in the respective composites, Figure 6c and d. Nevertheless, the kind of metal cation had an impact on the oxidation temperature and therefore on the quality of the CNs produced, as the DTA results indicate an oxidizing temperature of 586 °C for nickel-grown CNs and 553 °C for iron-grown CNs, Figure 6e. For reasons of comparison, Figure 6a and e show the thermogravimetric response of a clay−amorphous carbon composite prepared according to the literature,[35] which, as expected, undergoes oxidative degradation at a much lower temperature than CNs (461 °C).

A final remark refers to the effect of metal catalyst load and of gas flow time on the CN yield. In Table 1 the carbon content of several MNTNi2%−CN and MNTNi5%−CN composites, as calculated from TG measurements, is cited for different times of reaction and the related data are shown schematically in Figure 7. It is observed that during the first ∼5−10 min no carbon deposition occurs, while during the next 15 min a steep rise in the yield takes place regarding especially the 5% Ni-loaded clay. After 30 min of reaction the CN production practically ends for the MNTNi2%−CN sample, while for MNTNi5%−CN the yield continues to increase but at a lower rate. Finally, a reaction time of 20

(34) Qingwen, L.; Hao, Y.; Yinchun, Y.; Jin, Z.; Zhongfan, L. *J. Phys. Chem. B* **2002**, *106*, 11085.
(35) Bakandritsos, A.; Steriotis, Th.; Petridis, D. *Chem. Mater.* **2004**, *16*, 1551.
(36) Bahlawane, N. *Thin Solid Films* **2001**, *396* (12), 126.

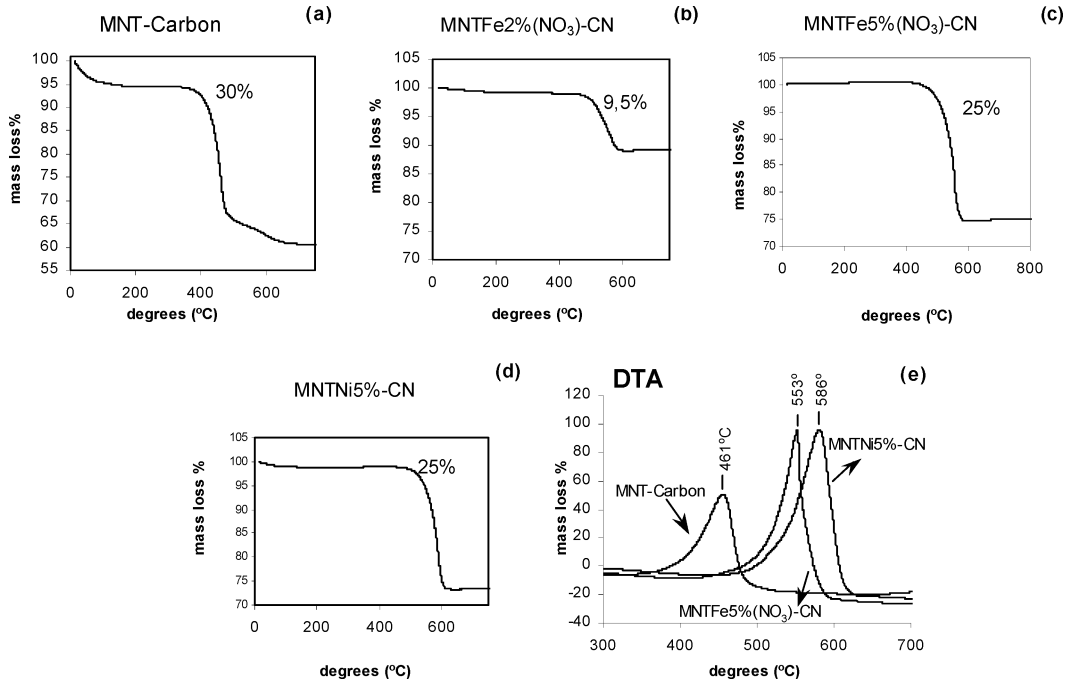

Figure 6. TG diagrams of (a) clay/amorphous carbon composite, (b) MNTFe2%(NO_3)−CN, (c) MNTFe5%(NO_3)−CN, and (d) MNTNi5%−CN, and (e) DTA curves of amorphous carbon supported on clay, MNTFe5%(NO_3)−CN, and MNTNi5%−CN composites.

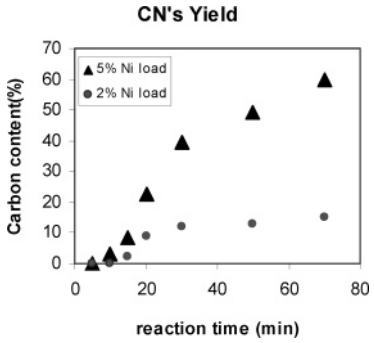

Figure 7. Plot of the carbon content (CNs) of the obtained MNTNi2%−CN and MNTNi5%−CN composites versus the time of the catalytic reaction.

Table 1. Carbon Contents of MNTNi2%−CN and MNTNi5%−CN Composites for Various Times of Carbon Deposition at 700 °C and the Oxidizing Temperature of CNs

duration (min)	carbon content (%w/w)		oxidizing temp. (°C)
	MNTNi2%−CN	MNTNi5%−CN	MNTNi5%−CN
5	0	0	
10	0	2.9	554
15	1.9	8.6	564
20	9.2	22.5	586
30	12.0	39.4	565
50	12.9	49.0	562
70	13.0	60	559

min is considered as the best time for CN growth because it combines an adequate CN yield with retention of the swelling, intercalation, and ion exchange properties of the clay, as previously discussed.

Mössbauer Spectroscopy. Mössbauer spectroscopy enables the study and understanding of the role of iron in the clay substrate during the CN synthesis. The spectrum of starting montmorillonite treated with $Fe(NO_3)_3$ exhibits a main peak (96%), Figure 8a, corresponding to ferric cations from either intercalated or structural iron. The minor peak (4%) arises from structural Fe(II) cations. After carbon deposition at 700 °C in the reducing C_2H_2 atmosphere, the nature of iron atoms has significantly altered. The distribution of the postreaction iron components is 87% Fe(II) comprising two paramagnetic doublets, 5% Fe(III) comprising a third paramagnetic doublet, and the remaining 8% comprising a singlet with isomer shift −0.12 mm/s (Table 2), indicating the formation of the metastable fcc (face centered cubic) iron phase, probably austenite (a γ-Fe form with carbon atoms in the lattice interstitial positions). The fcc phase is not stable at room temperature and below 1000 K transforms to the bcc phase (body centered cubic) called martensite, which appears as a magnetic sextet in Mössbauer spectra. Stabilization of the fcc phase at room temperature has been observed when the particle size is constricted to nano-dimensions inside other matrixes.[37,38] Similarly, in the present case, entrapment of very small austenite particles in the mineral's super-lattice appears to be the reason for its stabilization.

Regarding the two paramagnetic doublets of Fe(II), we propose that they arise from migration of the divalent iron to the vacant octahedral sites of the clay lattice during the reductive heat treatment.[39,40] (A detailed elaboration on the fate of iron species during carbon deposition on montmorillonite will be submitted for publication soon.) Formation of iron oxides is excluded as no magnetic hyperfine structure (sextet) is observed in the temperature spectrum (Figure 8b). In addition, iron carbides are not detected, in agreement with the XRD data. On the contrary, the Mössbauer spectrum of a clay−CN composite derived from an $FeCl_3$-exchanged clay clearly shows the abundant formation of a magnetic iron carbide phase[23] (sextet in Figure 8c). Since the starting clay

(37) Gómez-Polo, C.; Hernando A.; Ghannami, M. El. *J. Magn. Magn. Mater.* **1998**, *187*, 117.
(38) Crespo, P.; Hernando. A.; Yavari, R.; Drbohlav, O.; García Escorial, A.; Barandiaran, J. M.; Orue, I. *Phys. Rev. B.* **1993**, *48*, 7134.
(39) Karakassides, M. A.; Madejová, J.; Arvaiová, B.; Bourlinos, A. B.; Petridis, D.; Komadel, P. *J. Mater. Chem.* **1999**, *9*, 1553.
(40) Luca, V.; Cardile, C. M. *Clays and Clay Miner.* **1989**, *37* (4), 325.

Table 2. Mössbauer Parameters[a]

	MNTFe2%(NO_3)				MNTFe2%(NO_3)−CN				MWCNs					
	δ	Γ	ΔE_Q	P	δ	Γ	ΔE_Q	P	δ	Γ	ΔE_Q	H_{hf}	DH	P
Fe^{3+}	0.35	0.52	0.62	79.7	0.41	0.3	1.4	5						
Fe^{3+}	0.3	0.58	1.08	16.4										
Fe^{2+}	1.23	0.44	2.6	3.8	1.26	0.38	2.4	27.4						
Fe^{2+}					1.19	0.64	1.82	55.4						
γ-Fe					−0.12	0.3		7.8						
Fe_3C									0.33	0.4	0.03	254	9	100

[a] δ: Isomer shift (mm/s, respective to α-Fe). ΔE_Q: Quadrupole splitting (mm/s). Γ: Line width (mm/s). H_{hf}: Hyperfine field (kOe). P: Proportion (%).

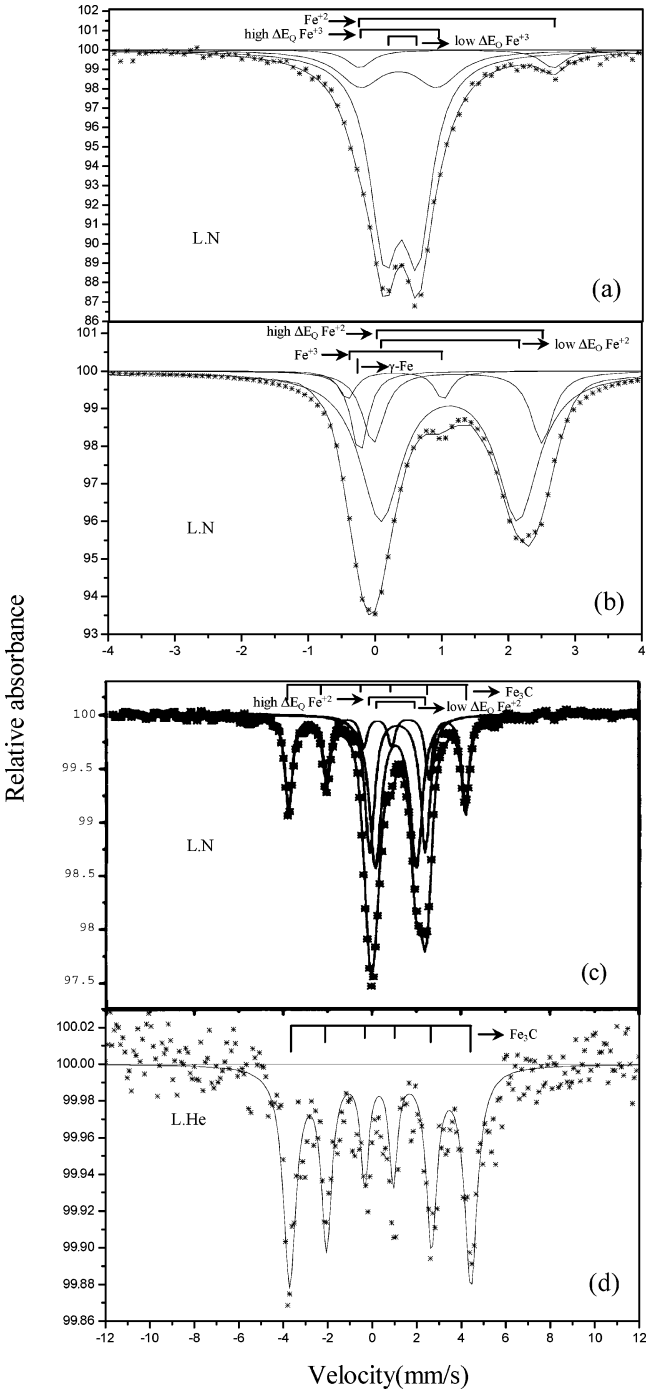

Figure 8. Mössbauer spectra at liquid nitrogen temperature of (a) clay loaded with $Fe(NO_3)_3$, (b) the clay−CN composite, MNTFe2%(NO_3)−CN, (c) the clay−CN composite MNTFe2%(Cl)−CN (from ref 23), and (d) pure MWCNs after demineralization of MNTFe2%(NO_3)−CN.

precursors MNTFe2%(Cl) and MNTFe2%(NO_3) were free from their counterions after the exchange reactions, the

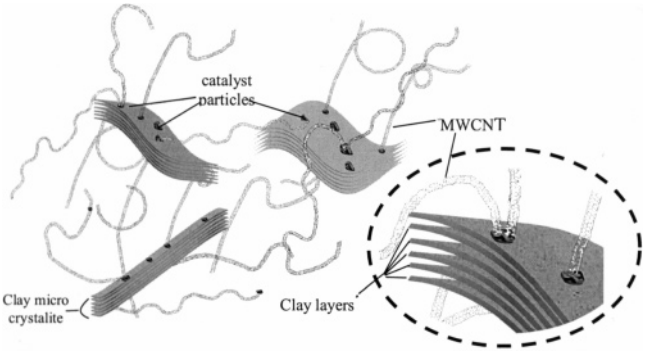

Figure 9. Tentatives chematic representation of the microstructure in the final clay−CN composites.

observed behavior probably stems from the different iron oxyhydroxide species (α, β, and γ forms) that are formed upon hydrolysis of the initially added ferric salt.[41] Iron oxyhydroxides behave differently upon thermal treatment and give different iron oxides.[42] In turn, iron oxides (hematite, magnetite, maghemite, wustite ϵ-Fe_2O_3) when subjected to a reductive and carburizing atmosphere undergo different processes upon their interaction with carbon atoms and their transformation to carbides.[43]

It is also interesting to note that although no iron carbide phase was detected in the clay−CN composite, the Mössbauer spectrum of pure MWCNs after dissolution of the clay points to the presence of Fe_3C, entrapped in the CN walls. The amount of this component is ∼1‰ with respect to the total iron amount in the composite MNTFe2%(NO_3)−CN and for this reason remained undetected in the spectrum of the composite. The very small Fe_3C content, according to Mössbauer results, shows that the obtained MWCNs are to a good extent in a satisfactory pure state.

Conclusions

On the basis of the discussed results we present in Figure 9 a tentative view of the clay−CN microstructure. The clay layers are not finely dispersed in the clay−CN mass, but form crystallites with parallel stacking. Metal nanoparticles immobilized on the surfaces or at the edges of clay stacks (tactoids) are the catalytic sites for MWCN development.

In summary, the main contribution of the present work refers to the conditions for optimizing the quality and yield of CNs grown on montmorillonite surfaces by examining

(41) Doelsch, E.; Rose, J.; Masion, A.; Bottero J.; Nahon, D.; Bertsch, P. M *Langmuir* **2000**, *16*, 4726.
(42) Ponce-Castaneda, S.; Martinez, J. R.; Palomares-Sanchez, S. *J. Sol−Gel Sc. Technol.* **2003**, *27*, 247.
(43) Bonnet, F.; Ropital, F.; Lecour, P.; Espinat, D.; Huiban, Y.; Gengembre, L.; Berthier Y.; Marcus, P. *Surf. Interface Anal.* **2002**, *34*, 418.

some important factors that affect the catalytic formation of CNs while at the same time maintaining the valuable properties of the parent mineral in the clay−CN composites. Nitrate metal salts supported on montmorillonite as catalyst precursors yielded CNs practically free of metal carbide impurities. In addition, the use of $Ni(NO_3)_2$ afforded CNs of high quality (low number of defects). Another interesting result is the correlation between the characteristics of the *002* reflection of MWCNs and the oxidizing temperature with the quality of the CNs produced. Moreover, the effect of flow time on carbon deposition was examined to attain composites combining a high CN content with preservation of the clay properties. Finally, the ability of the clay partner in the composites to undergo organo-modification and the facile wet intercalation of polyethylenoxide are promising results that pave the way for the synthesis of novel clay−CN−polymer nanocomposite materials.

CM0482131